<u>**Answers to Reviewers' Comments**</u>

Referee #1,

I have checked the response and the revised manuscript. To me, the reply message is clear and informative. My overall impression is that the revised manuscript is improved. The previous main concerns have been widely addressed. However, in my opinion, there may be just three minor issues that could be addressed.

<u>**Minor comments**</u>

1. The reply message (2.1 A.) shows the justification of the order selected for different filters (e.g., the third order selected for the Butterworth filter, the sixth order selected for the FIR1 filter), but this information is not indicated in the revised manuscript. As far as I am concerned, it is better to include this message in the revised manuscript.

Reply.   As per the suggestion of the reviewer, we have incorporated the justification of the selection of order in the revised manuscript.

2. Similar to the above comment, it is also better to include the reply message of 2.3 A. in the revised manuscript, which is about the clarification of outliers or data gaps.
Reply. We have incorporated the clarification of outliers and data gaps in the revised manuscript.

3. According to the reply message in 2.7 A., the statistical significance test is not used in this paper, and the authors haven't yet introduced the proposals about how

to determine the statistical significance with a large number of hodographs. Therefore, I would suggest that the authors delete or modify the last sentence of the summary section, in order to eliminate the redundant information and potential confusion.

Reply. The last sentence from abstract, section 3.3 and in the summary section "but a large number of hodographs are needed to confirm it with statistical significance" have been deleted in the revised manuscript.

Comment on revised version of "Retrieving characteristics of Inertia Gravity Wave parameters with least uncertainties using hodograph method" by Gopa Dutta et al.

Referee #2, Vladimir Gubenko

This paper presents an attempt to overcome the inconsistency of hodograph method when retrieving the internal wave parameters from radiosonde measurements. It seems to me, the description of scientific methods and theoretical expressions used for calculations of wave characteristics and their uncertainties **is not satisfactory and needs to be strongly improved**. **Authors of this paper should better learn the basic equations and hodograph method for internal gravity waves.** I think that this **paper is not acceptable for publication in the journal with a high standard "Atmospheric Chemistry and Physics"** in its present form. For this reason, I would advice **MAJOR REVISION.**

Major Comments:

1. Page 3, line 27. Authors would like to leave in the text of revised version their polarization Eq. (1) and following designations: u' are zonal wind perturbations and v' are meridional wind perturbations (see author's answers to my comments). Of course, authors may choose any designations for variables, but **in this case your Eq. (1) is not polarization Equation for the values u' and v'! In reality, your Eq. (1) is polarization Equation for the parallel and perpendicular perturbation components** of wave-induced horizontal wind speed to the wave propagation direction [see for details, for example, Gubenko et al. (2008, JGR, p. 2); Gubenko et al. (2011, AMT, p. 2155); Gubenko et al. (2012, Cosmic Res., p. 22)].

For the general case of an inertia gravity wave with intrinsic frequency ω, propagating in an atmosphere with Coriolis parameter *f*, the meridional (*v'*) and zonal (*u'*) wind oscillations differ in amplitude and phase, and are related through the following expression (see formula (2) on page 513 of Eckermann and Vincent (1989), or Gossard and Hooke (1975)):

$$v' = \frac{(l/k)[1 - i(f/\omega)(k/l)]u'}{[1 + i(f/\omega)(l/k)]} = \frac{(l/k) - i(f/\omega)}{1 + i(f/\omega)(l/k)}u' = \frac{(\omega l - ifk)}{\omega k + ifl}u' \qquad (1)$$

where *k* and *l* are the zonal and meridional components of the horizontal wavenumber vector, respectively. This formula implies elliptical wave polarization, with frequency dependent ellipse eccentricity of (*f* /ω). The phase motion of such an inertial gravity wave will have a horizontal component, lying along the major axis of this motion ellipse. **Only in the special case, for a zonally propagating wave (*l* = 0), our polarization Eq. (1) will coincide with polarization Eq. (1) of your manuscript.**

Unfortunately, the citation of Tsuda et al. (1994) is not the real argument, because this work contains the same mistakes as you do.

Reply: Following the referee's suggestion, we have gone through the seminal studies cited by him on IGW. Now, we understood our mistake in depicting the polarization equation (equation 1 in the manuscript), which correspond to special case i.e., when l=0. We have made changes accordingly in the revised manuscript.

2. Page 3, line 32. **You have not considered my early comments.** In the work of Gubenko et al. (2012, Cosmic Res., p. 23), the dispersion equation in the interval of intermediate intrinsic frequencies ($f^2 << \omega^2 << N^2$) is given: $|k| = \omega |m| / N$. This

equation assumes **only** linear wave polarization but nor elliptical wave polarization, because $f^2 << \omega^2$. **If you use your Eq. (3)** to calculate the value $/k/$, then calculated values of horizontal wave number $/k/$ **will be systematically overestimated by factor $(1 - f^2/\omega^2)^{-1/2}$**. This is connected with fact that **the appropriate dispersion equation for your case study** should be valid for internal waves both with low and with intermediate intrinsic frequencies ($f^2 < \omega^2 << N^2$). **The appropriate dispersion equation** has form (Gubenko et al. 2012, Cosmic Res., p. 23): $/k/ = (1 - f^2/\omega^2)^{1/2} \cdot \omega \, /m/ \, / \, N$.

For example, for ratio $f/\omega = 0.6$ (see your Table 2), one can find that $(1 - f^2/\omega^2)^{-1/2} = 1 / 0.8 = 125\%$. Here, we see the significant overestimation by 25% for the calculated value of $/k/$. This is not "small mistake" (see author's answers to my comments), **and the obtained results about horizontal wavelengths and wave numbers must be recalculated.**

Reply: We had actually used the proper equations suggested by the Dr. Gubenko. But we have also retained equation 3. Now we have removed equation 3. There is no over estimation of the parameters in the tables since we have calculated them by using equation 3 of the revised manuscript. We request the reviewer to check our earlier manuscript where we have calculated parameters using equation k=mω/N and the values projected in this manuscript and the previous one are already corrected.

3. Page 4, line 5. Your phrase **"Intrinsic periods of IGW obtained using equation (4) …"** is completely incomprehensible.

Reply: We thank the reviewer for projecting this mistake. We have corrected it in the revised manuscript.

4. The description **of Section 3.3 "Direction of wave propagation" is not satisfactory,** and it should be remade.

Reply: As per the suggestion of the reviewer we have clarified the direction of wave propagation in the revised manuscript.

Overall, we thank Dr. Gubenko for giving strong comments which helped to improve the quality of the paper reasonably.

References

Eckermann, S.D. and Vincent, R.A., 1989. Falling Sphere Observation of Anisotropic Gravity Wave Motions in the Upper Stratosphere over Australia. Pure Appl. Geophys. 130 (2/3), 509–532.

Gossard, E.E. and Hooke, W.H., 1975. Waves in the Atmosphere, Elsevier, Amsterdam.

Gubenko, V.N., Pavelyev, A.G., Andreev, V.E., 2008. Determination of the intrinsic frequency and other wave parameters from a single vertical temperature or density profile measurement. J. Geophys. Res. 113, D08109, doi:10.1029/2007JD008920.

Gubenko, V.N., Pavelyev, A.G., Salimzyanov, R.R., Pavelyev, A.A., 2011. Reconstruction of internal gravity wave parameters from radio occultation retrievals of vertical temperature profiles in the Earth's atmosphere. Atmos. Meas. Tech. 4, 2153–2162, doi: 10.5194/amt-4-2153-2011.

Gubenko, V.N., Pavelyev, A.G., Salimzyanov, R.R., Andreev, V.E., 2012. A method for determination of internal gravity wave parameters from a vertical temperature or density profile measurement in the Earth's atmosphere. Cosmic Res. 50, 21–31, doi: 10.1134/S0010952512010029.

Tsuda, T., Murayama, Y., Wiryosumarto, H., Harijono, S.W.B., Kato, S., 1994. Radiosonde observations of equatorial atmospheric dynamics over Indonesia, 2. Characteristics of gravity waves. J. Geophys. Res., 99, 10507-10516.

Retrieving characteristics of Inertia Gravity Wave parameters with least uncertainties using hodograph method

Gopa Dutta[1], P. Vinay Kumar[1] and Salauddin Mohammad[1]

[1]Vignana Bharathi Institute of Technology, Hyderabad 501301, India.

5   *Correspondence to*: Gopa Dutta (gopadutta@yahoo.com)

Abstract. We have analyzed time series of wind velocities measured with high resolution GPS-radiosonde ascents continuously for 120 h from Hyderabad with an interval of 6 h. Hodograph method has been used to retrieve the Inertia Gravity Waves (IGW) parameters. Background winds are removed from the time series by detrending whereas polynomials of different orders are removed to get the fluctuations from individual profiles. Butterworth filter is used to extract

10   monochromatic IGW component. Another filter Finite Impulse Response (FIR1) is tried in a similar manner to test the effects of filters in estimating IGW characteristics. Results reveal that the fluctuation profiles differ with the change of polynomial orders, but the IGW parameters remain same when Butterworth filter is chosen to extract the monochromatic wave component. FIR1 filter also produces acceptable results with a broader range. The direction of wave propagation ~~is~~ can be confirmed with additional temperature information ~~which needs a large number of hodographs for statistical significance~~.

15   **1 Introduction**

It is well documented that gravity waves of different scales play an important role in maintaining the large-scale circulation of the middle atmosphere. A large number of studies have been carried out to characterize these waves by using different techniques. A very common, established and standard procedure of characterizing Inertia Gravity Waves (IGW) with frequencies close to Coriolis frequency is by hodograph method (Guest et al., 2000; Ogino et al., 2006; Niranjan Kumar et

20   al., 2011). Radiosonde data of horizontal winds and temperature have been extensively used to study these waves (Tsuda et al., 2004; Vincent and Alexander, 2000; Gong et al., 2008; Chane-Ming et al., 2010, 2014; Murphy et al., 2014; Kramer et al., 2015). Nastrom and VanZandt (1982) reported good accuracy in gravity wave parameters derived using balloon measurements since balloons have good aerodynamic responses. In a simulation study Wei and Zhang (2014) have demonstrated that gravity waves with different frequencies and generated by different sources like jet-imbalance and

25   convection can coexist together. The popular hodograph method demands the presence of a single coherent wave in the fluctuation profiles and does not yield good result when a mixture of various frequencies are present. The gravity wave

parameters extracted by hodograph method might also be inaccurate when multiple waves are present in the data (Eckermann and Hocking, 1989).

Hodograph method is based on linear theory of gravity waves whereas the dynamics of the flow is more complex and non-linear which introduces some uncertainties in their interpretations. There are several sources of errors in this method which have been described in Zhang et al., (2004). These authors compared the gravity wave characteristics obtained using hodograph method with the values derived from 4D output of their simulation study. A narrow bandwidth filter used by them to extract the fluctuations of a near-monochromatic wave resulted in large uncertainties in the horizontal wavelength which got reduced for waves with shorter vertical wavelengths. Even the spatial variations of the wave characteristics were found to be large. Moreover, since the hodographs are quite variable, a large number of hodographs (profiles) are required to get accurate results of gravity wave parameters with some statistical significance (Hall et al., 1995). This defeats the very advantage of the hodograph method which is capable of retrieving GW parameters from a single set of vertical profiles of zonal and meridional winds.

The present paper attempts to overcome the inconsistency of hodograph method in delineating the characteristics of IGW from velocity fluctuations obtained with radiosonde measurements.

2 Experiment and Data

An intensive campaign with high resolution (i-Met, USA) GPS–radiosonde flights was carried out from the campus of India Meteorological Department (IMD), Hyderabad (17.4 ºN, 78.5 ºE) with four flights a day at an interval of 6 h for 5 consecutive days (20 flights) between 30 April and 4 May, 2012 to study the characteristics of IGW. The timings of the flights were 05:30, 11:30, 17:30 and 23:30 LT. The accuracy of wind and temperature measurements provided by the manufacturer is ± 1 ms^{-1} and ± 0.2 K respectively. There was one data gap at 11:30 LT on 4 May, 2012 which was linearly interpolated to get continuous time series of wind velocities. High resolution (~4 – 10 m) wind data obtained directly from balloon flights were first sorted in ascending order of height since the balloons occasionally drift downwards by a few meters. The wind profiles were then interpolated vertically to have a constant height resolution of 50 m. This method is useful to smooth the profiles and to maintain a good resolution in height. The profiles were then visually inspected for outliers. Only four outliers could be identified out of 20 profiles which were removed and the gaps were filled up by linear interpolation with height.

3 Analysis and Discussion

3.1 Time series analysis

IGW periods over low latitudes are quite large which makes their observations difficult by using common spectral analysis method. The normal procedure to find the frequency/period of an atmospheric wave is to have a continuous time series data with appropriate data gaps and subject it to Fast Fourier Transform (FFT) technique. The minimum length of data required for FFT analysis is double the period of the wave (Nyquist frequency) to be identified. Keeping this in mind, experiments were conducted as mentioned in section 2 to obtain wind velocities and temperatures continuously for 120 h with a regular interval of 6 h since the IGW period over Hyderabad is ~40 h and the data contains three cycles of the wave which satisfies the criterion of FFT technique. This time series data is capable of identifying IGW period after proper filtering and using spectral analysis method. The filtered time series data is considered as reference data for rest of the analyses.

We have used two types of filters. Butterworth filter and Finite Impulse Response (FIR) filter in the present work. Butterworth filter belongs to the Infinite Impulse Response (IIR) group of filters. It is a type of signal processing filter designed to have a very flat frequency response in the pass band with a monotonic amplitude response. FIR filters can be reliably designed with linear phase that prevents distortion. These filters can be easily implemented but with the disadvantage that they often require a much higher filter order than IIR filters to achieve a good level of performance. The details of these filters are available in Butterworth (1930) and Lake (1980). The order of the filter refers to the number of components that affect the steepness or shape of the filter's frequency response. As the order of the filter increases, the cut-off becomes sharper, but the length of the data should be at-least 3 times the filter order. The length of our data is 20 (time-wise). So which restricts the maximum order of the filter which we couldto be choosechosen isas 6. A Butterworth filter of order 3 is more efficient than a 6th order FIR1 filter.

3.1.1 Hodograph of wind perturbations using Butterworth filter

-The continuous zonal and meridional wind datasets are detrended (linear trend removed) to obtain time series of wind fluctuations. A third order Butterworth filter with a band-pass between 36 and 44 h is applied to the wind perturbations to retrieve the IGW fluctuations with zero phase distortion. The sufficiently wide band of the time filter is helpful to reduce the Doppler shift of IGW frequency (Niranjan Kumar et al., 2011). Ehard et al., (2015) also recommended the usage of Butterworth filter in extracting gravity waves over a wide range of periods from temperature perturbations measured by lidar. The filtered horizontal winds at particular heights are depicted in Fig. 1a – 1d which show the presence of IGW with a period of ~ 40 h. FFT analyses carried out with filtered wind fluctuations also reveal the presence of a clear monochromatic wave of the same period (Fig. 1e – 1h) which satisfies the requirement of hodograph method.

Hodographs plotted with this time-wise filtered zonal and meridional wind perturbations (u_{ew}', v_{ns}') are found to be quite noisy and it is difficult to identify proper closings. The fluctuation profiles are, therefore, further band-pass filtered using a

3

Butterworth filter with a cut-off at 1.5 – 4 km which produced proper elliptic hodographs. The number of proper hodographs obtained from 20 pairs of vertical profiles of u_{ew}' and v_{ns}' are 124. For the general case of an inertia gravity wave with intrinsic frequency ω, propagating in an atmosphere with Coriolis parameter f, the meridional (v') and zonal (u') wind oscillations differ in amplitude and phase, and are related through the following expression (Eckermann and Vincent (1989), Gossard and Hooke (1975))

$$v' = \frac{(l/k)[1-i(f/\omega)(k/l)]u'}{[1+i(f/\omega)(l/k)]} \qquad\qquad (1)$$

where k and l are the zonal and meridional components of the horizontal wavenumber vector, respectively. This formula implies elliptical wave polarization, with frequency dependent ellipse eccentricity of (f /ω). The phase motion of such an inertial gravity wave will have a horizontal component, lying along the major axis of this motion ellipse. Assuming a zonally propagating wave ($l = 0$), equation (1) reduces to,

~~A few IGW parameters have been extracted assuming linear dispersion relations (Tsuda et al., 1994). The intrinsic wave frequency (ω) is calculated from the ratio of minor to major axes of the ellipse.~~

$$\frac{v'}{u'} = -i\left(\frac{f}{\omega}\right) \qquad\qquad (\text{1}\underline{2})$$

~~where f is the inertial frequency and u′, v′ are the amplitudes of wind velocity fluctuations due to gravity wave. f is computed as~~

$$f = \frac{\sin\varphi}{1/_2 day} \; cycles/sec \qquad\qquad (2)$$

~~where φ is the latitude of the place.~~ A few IGW parameters have been extracted using equation (2). The horizontal wave number k ~~is found using the relation~~

$$k = m\omega/N \qquad\qquad (3)$$

~~N being the Brunt – Väisälä frequency and m is vertical wave number. Equation (3) is valid for $N \gg \omega \gg f$ (Fritts and Alexander, 2003). Gubenko et al., (2012) has reported that the dispersion equation which is valid~~ for internal waves with both low and intermediate intrinsic frequencies ($f^2 < \omega^2 \ll N^2$) is given by the following equation (Fritts and Alexander, 2003; Gubenko et al 2012):

$$k = \left(1 - \frac{f^2}{\omega^2}\right)^{1/2} \frac{m\omega}{N} \qquad\qquad (\text{4}\underline{3})$$

Intrinsic periods of IGW obtained using equation (4̶2) from hodographs range between 20 – 28 h which are less than the inertial period of Hyderabad and belongs to ~~this~~ the intermediate range. The vertical and horizontal wavelengths inferred from the hodographs are between 2.0 to 2.8 km and ~~between~~ 569 – 1171 km respectively.

3.1.2. Hodographs using FIR1 filter

Next we chose a different filter FIR1 of order 6 to test the effect of filtering on hodograph method since the vertical wavelength and intrinsic frequency are reported to be highly vulnerable to the filter used (Zhang et al., 2004). We followed the same procedure to delineate the IGW parameters as described in section 3.1.1 but by using FIR1 filter. The detrended

and time-wise filtered horizontal wind profiles at a few heights and the corresponding FFT peaks are illustrated in Fig. 2a – 2d and 2e – 2h respectively. Both the time variation of wind fluctuations and the FFT peaks do not show distinct IGW periods. The frequency responses of Butterworth filter of 3rd order and FIR1 of 6th order are shown in Fig. 3. The Butterworth filter shows a sharp cut-off and also has the advantage of producing good result with a much lower filter order than the corresponding FIR1 filter. A few hodographs plotted with horizontal wind perturbations using both the filters are displayed in Fig. 4a – 4d. North is denoted by 0° in the hodographs and the angle increases clockwise. Clockwise rotation of hodograph indicates upward energy propagation in the northern hemisphere. The IGW parameters derived from these hodographs are listed in Table 1. The ranges of horizontal wavelength, vertical wavelength and intrinsic period are observed to be broader using FIR1 filter compared to those obtained using Butterworth filter.

3.2. Height series analyses

Hodographs are generally plotted with the fluctuations derived from data of individual sounding by removing polynomials of 1st or 2nd order. We treated the measured vertical profiles of zonal and meridional winds as single individual set (not time series) and approximated the backgrounds by polynomials of different (2 to 9) orders. Fig.5 depicts the different fits and the corresponding wind profiles. The fluctuation profiles obtained by removing polynomials of 4, 5 and 6 orders show close agreements whereas appreciable differences could be noticed for others (figure not shown). These fluctuation profiles are then subjected to different filtering process and hodographs are plotted. They are consequently analyzed to derive IGW parameters.

3.2.1 Hodographs using Butterworth filter

The perturbation profiles are filtered with a 3rd order Butterworth filter height-wise to retain IGW oscillations with short vertical wavelengths (1.5 – 4 km). IGW parameters obtained from the hodographs plotted with these fluctuations match extremely well with those described in section 3.1.1

3.2.2 Hodographs using FIR1 filter

The individual profiles of winds and temperature are then analyzed in a similar manner as mentioned in section 3.2.1 but by using FIR1 filter with height instead of Butterworth filter. The perturbation profiles (after removing backgrounds with different order polynomials) and the filtered fluctuation profiles using both Butterworth and FIR1 filters are shown in Fig. 6a – 6c and 6d – 6f for both the wind components, respectively. It is clearly observed that the Butterworth filter can extract the monochromatic IGW fluctuations very efficiently. The retrieved IGW parameters retain same numerical values (except after decimal points) irrespective of the background removals. Results obtained with FIR1 filter also belong to the same range but with a broader band which is illustrated in Table 2 for different orders.

3.3. Direction of wave propagation

The direction of horizontal wave propagation is parallel to the major axis of the $u_{ew}' - v_{ns}'$ hodograph (ellipse) which is uncertain by 180º. This uncertainty can be removed with the help of additional temperature information. Temperature perturbation profiles are obtained by removing 5th order polynomial fits from the simultaneous temperature profiles and filtering them height-wise with a band-pass Butterworth filter between 1.5 and 4 km. In-phase wind is calculated as $U\cos\theta$ where U is the total wind and θ is the corresponding orientation angle of the $u_{ew}' - v_{ns}'$ hodograph (Fig. 4a - d). A few hodographs plotted with in-phase winds and temperature fluctuations are illustrated in Fig. 7 (a –d) which help in resolving the ambiguity ~~to determine the~~ of wave propagation direction (Hu et al., 2002). If the rotation of in-phase wind and temperature perturbation hodograph is clockwise, the direction (angle) of horizontal wave propagation will be the same as the orientation angle determined by $u_{ew}' - v_{ns}'$ hodograph. If the rotation is counter clockwise, it indicates that the propagation direction will be opposite to the orientation angle i.e. orientation angle +180°. As an example, let us consider the hodograph depicted in Fig. 4a. The orientation angle of the major axis of the ellipse is 154.4°. The propagation direction can, therefore, be 154.4° or 154.4° +180°. The corresponding in-phase wind and temperature fluctuation hodograph (Fig. 7a) rotates clockwise confirming the propagation direction to be south-east (154.4°). The unambiguous direction of propagation of IGW is observed to be south-east (58%) in this ~~analysis~~study. It is necessary to analyze a large number of hodographs to finalize the direction of propagation. ~~with some statistical significance.~~

4 Summary

Balloon borne experiments have been conducted for five days with an interval of 6 h to characterize IGW using hodograph method. The method is helpful in identifying low-frequency IGW but suffers from several uncertainties. We have utilized the time series of wind fluctuations to extract IGW component by filtering and confirmed it with spectral analysis. Results obtained by using Butterworth and FIR1 filters are compared. A band-pass Butterworth filter with a sharp cut-off is found to isolate the monochromatic IGW component very efficiently. Backgrounds of individual wind profiles have been approximated with polynomials of different orders when the perturbation profiles show reasonable differences. The differences are observed to get reduced when Butterworth filter is used to isolate the IGW components, whereas differences still persist with FIR1 filter. IGW parameters delineated from the corresponding hodographs using the former filter agree extremely well for different order polynomial removals. Results obtained with FIR1 filter also show reasonable agreement but with a broader range. Filtering appears to be of great importance in removing uncertainties of hodograph method. The unambiguous direction of wave propagation can be ascertained using additional and simultaneous temperature information. ~~but a large number of hodographs are needed to confirm it with statistical significance~~.

References

Butterworth, S.: On the theory of filter amplifiers, Experimental wireless and the wireless engineer, 7, 536-541, 1930.

Chane-Ming, F., Chen, Z., and Roux, F.: Analysis of gravity-waves produced by intense tropical cyclones, Annales Geophys., 28, 531-547, 2010.

Chane-Ming, F., Ibrahim, C., Barthe, C., Jolivet, S., Keckhut, P., Liou, Y.-A., and Kuleshov, Y.: Observation and a numerical study of gravity waves during tropical cyclone Ivan (2008), Atmos. Chem. and Phys., 14, 641–658, 2014, doi:10.5194/acp-14-641-2014, 2014.

Eckermann, S. D., and Hocking, W. K.: Effect of superposition on measurements of atmospheric gravity waves: a cautionary note and some reinterpretations, J. Geophys. Res., 94, 6333-6339, 1989.

Eckermann, S.D. and Vincent, R.A.: Falling Sphere Observation of Anisotropic Gravity Wave Motions in the Upper Stratosphere over Australia. Pure Appl. Geophys. 130 (2/3), 509–532, 1989.

Ehard, B., Kaifler, B., Kaifler, N., and Rapp, M.: Evaluation of methods for gravity wave extraction from middle-atmospheric lidar temperature measurements, Atmos. Meas. Tech., 8, 46454655, doi:10.5194/amt846452015, 2015.

Fritts, D. C., and Alexander M. J.: Gravity wave dynamics and effects in the middle atmosphere, Rev. Geophys., 41(1), 1003, doi:10.1029/ 2001RG000106, 2003.

Gossard, E.E. and Hooke, W.H.: Waves in the Atmosphere, Elsevier, Amsterdam, 1975.

Gong, J., Geller, M. A., and Wang, L.:Source spectra information derived from U.S high-resolution radiosonde data, J. Geophys. Res., 113, D10106, doi:10.1029/2007JD009252, 2008.

Gubenko, V. N., Pavelyev, A. G., Salimzyanov, R. R., and Andreev, V. E.: A method for determination of internal gravity wave parameters from a vertical temperature or density profile measurement in the Earth's atmosphere, Cosmic Res., 50 (1), 21-31, 2012.

Guest, F., Reeder, M. J., Marks, C. J., and Karoly, D. J.: Inertia-Gravity wave observed in the lower stratosphere over Macquarie Island, J. Atmos. Sci., 57, 737-752, 2000.

Hall, G. E., Meek, C. E., and Manson, A. H.: Hodograph analysis of mesopause region winds observed by three MF radars in the Canadian prairies, J. Geophys. Res., 100, 7411-7421, 1995.

Hu, X., Liu, A. Z., Gardner, C. S., and Swenson, G. R.: Characteristics of quasi-monochromatic gravity waves observed with Na lidar in the mesopause region at Starfire Optical Range, NM, Geophys. Res. Lett., 29 (24), doi:10.1029/2002GL014975, 2002.

Kramer, R., Wüst, S., Schmidt, C., and Bittner, M.: Gravity wave characteristics in the middle atmosphere during the CESAR campaign at palma de Mallorca in 2011/2012: Impact of extratropical cyclones and cold fronts, J. Atmos. Sol. Terr. Phys., 128, 8-23doi:10.1016/j.jastp.2015.03.001, 2015.

Lake, R.: Programmes for digital signal processing, IEEE Xplore, DOI: 10.1109/MSP.1980.237616, 1980.

Murphy, D. J., Alexander, S. P., Klekociuk, A. R., Love, P. T., and Vincent, R. A.: Radiosonde observations of gravity waves in the lower stratosphere over Davis, Antarctica, J. Geophys. Res., 119, 11,973–11,996, 10.1002/2014 JD022448, 2014.

Nastrom, G. D., and VanZandt, T. E.: An analytical study of nonlinear responses of rising balloons in horizontal winds, J. Appl. Meteorol., 21, 413-419, 1982.

Niranjan Kumar, K., Ramkumar, T. K., and Krishnaiah, M.: MST radar observation of inertial-gravity waves generated from tropical cyclones, J. Atmos. Sol. Terr. Phys., 73, 1890-1906, doi:10.1016/j.jastp.2011.04.026, 2011.

Ogino, S. Y., Sato, K., Yamanaka, M. D., and Watanabe, A.: Lower stratospheric and upper-tropospheric disturbances observed by radiosondes over Thailand during January, 2000, J. Atmos. Sci., 63, 3437-3447, 2006.

Tsuda, T., Ratnam, M. V., May, P. T., Alexander, M. J., Vincent, R. A., and MacKinnon, A.: Characteristics of gravity waves with short vertical wavelengths observed with radiosonde and GPS occultation during DAWEX (Darwin Area Wave Experiment), J. Geophys. Res., 109, D20S03, doi:10.1029/2004JD004946, 2004.

~~Tsuda, T., Murayama, Y., Wiryosumarto, H., Harijono, S. W. B., and Kato, S.: Radiosonde observations of equatorial atmospheric dynamics over Indonesia, 2. Characteristics of gravity waves. J. Geophys. Res., 99, 10507-10516. 1994.~~

Vincent, R. A., and Alexander, M. J.: Gravity wave in the tropical lower stratosphere: An observational study of seasonal and inter-annual variability, J. Geophys. Res., 105, 17971-17982, 2000.

Wei, J., and Zhang, F.: Mesoscale gravity waves in moist baroclinic jet–front systems. J. Atmos. Sci., 71, 929–952, doi:10.1175/JASD130171.1, 2014.

Zhang, F., Wang, S., and Plougonven, R.: Uncertainties in using the hodograph method to retrieve gravity wave characteristics from individual soundings, Geophys. Res. Lett., 31, L11110, doi:10.1029/2004GL019841, 2004.

Figure Captions

Figure 1. Time series of filtered (Butterworth filter) fluctuations (ms^{-1}) of zonal and meridional winds (a – d) and corresponding FFT spectra (e – f) at a few heights.

Figure 2. Same as in Figure 1 but with FIR1 filter.

Figure 3. The filter responses of Butterworth (a) and FIR 1(b) filters.

Figure 4. Hodographs of horizontal wind fluctuations (ms^{-1}) obtained using Butterworth (a, b) and FIR1 (c, d) filters. An open circle and a solid circle in each hodograph indicate the lowest and highest altitudes, respectively. The thin curves represent the elliptical fits.
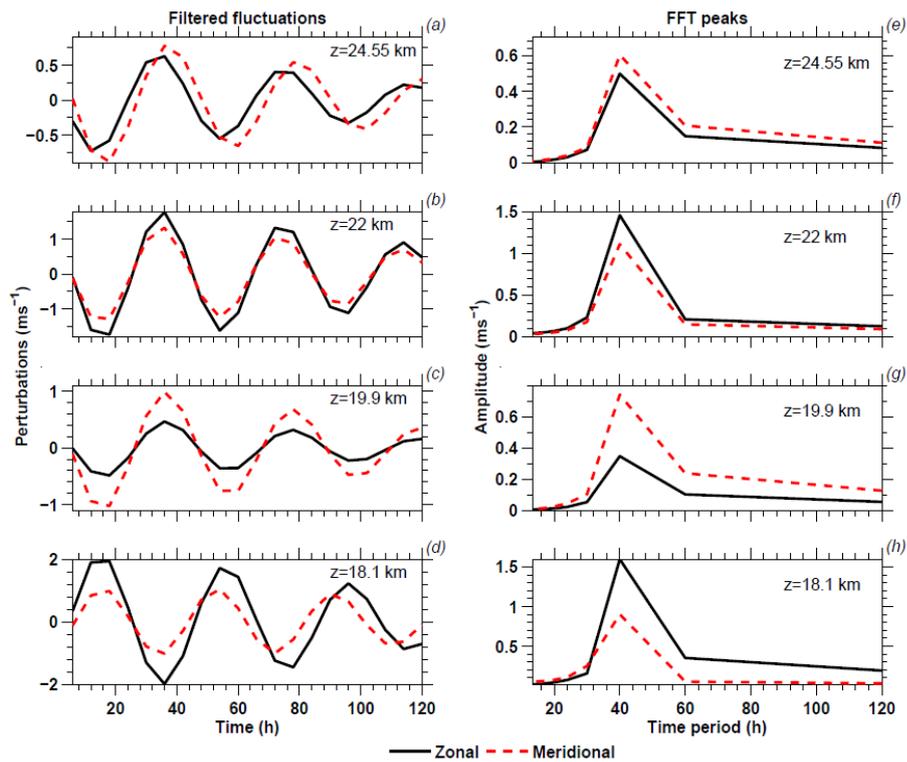
Figure 5. Profiles of zonal and meridional winds (ms^{-1}) and their fits with different orders.

Figure 6. Upper panel: Vertical profiles of zonal wind fluctuations (ms^{-1}) after approximating the backgrounds with different order (2nd – 9th) polynomials (a) and filtering height-wise with Butterworth filter (b) and FIR1 filter (c). **Lower panel:** Same as upper panel but for meridional wind fluctuations.

Figure 7. Hodographs of in-phase wind (ms^{-1}) verses temperature fluctuations (K) obtained using Butterworth (a, b) and FIR1 (c, d) filters. An open circle and a solid circle in each hodograph indicate the lowest and highest altitudes, respectively. The thin curves represent the elliptical fits.

Figure 1: Time series of filtered (Butterworth filter) fluctuations (ms⁻¹) of zonal and meridional winds (a – d) and corresponding FFT spectra (e – f) at a few heights.
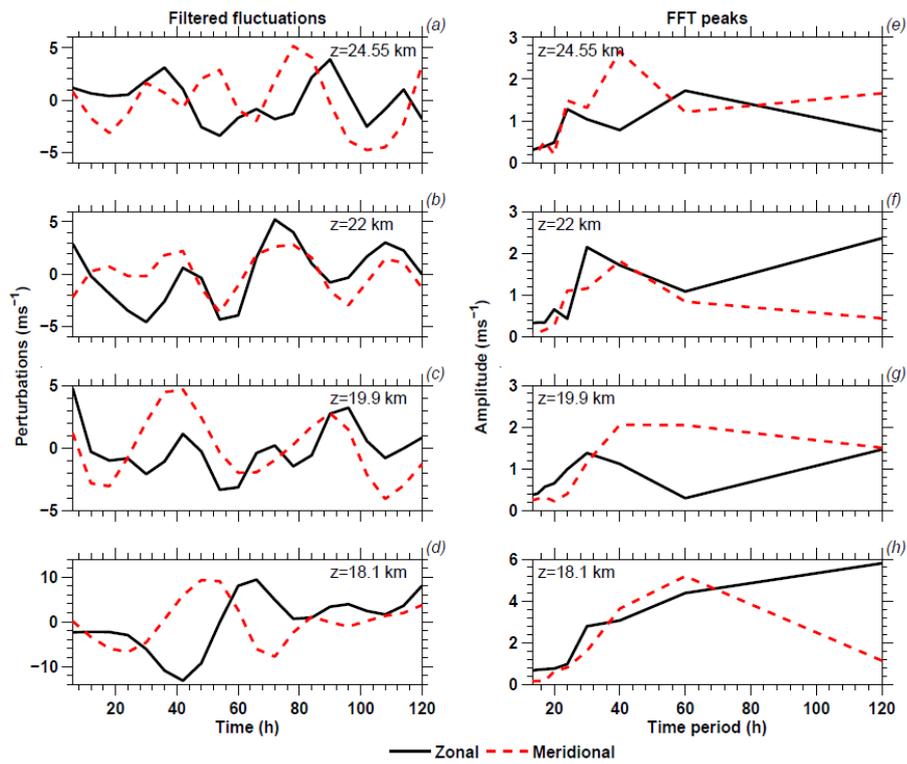
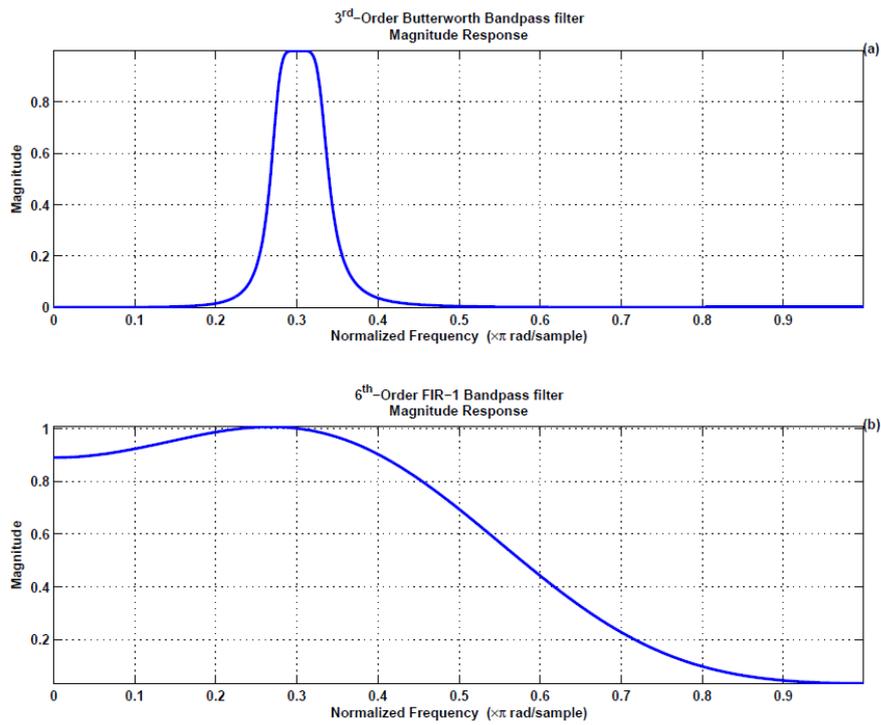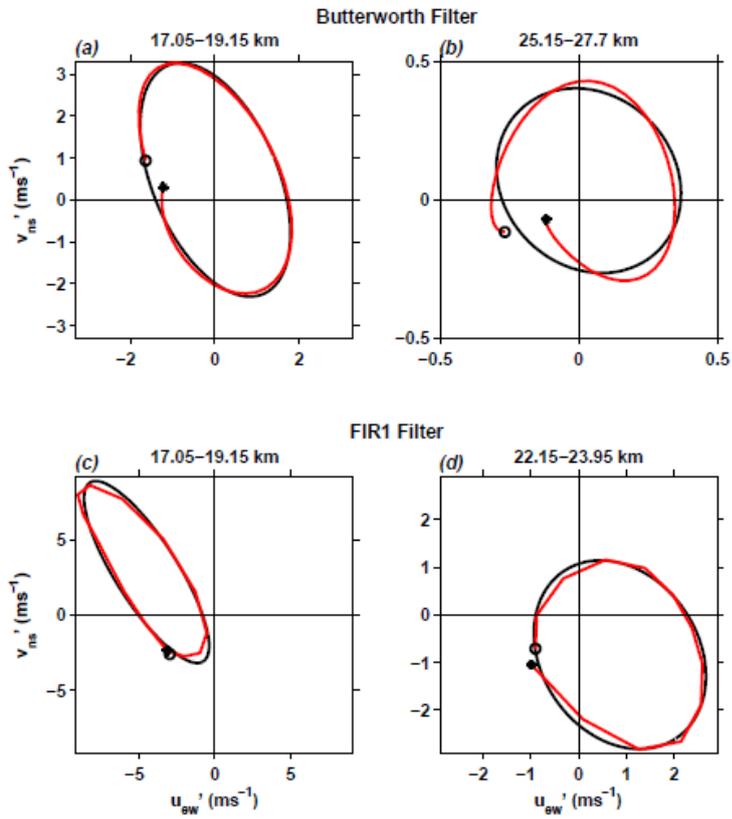**Figure 2: Same as in Figure 1 but with FIR1 filter.**

Figure 3: The filter responses of Butterworth (a) and FIR 1(b) filters.

Butterworth Filter

(a) 17.05–19.15 km

(b) 25.15–27.7 km
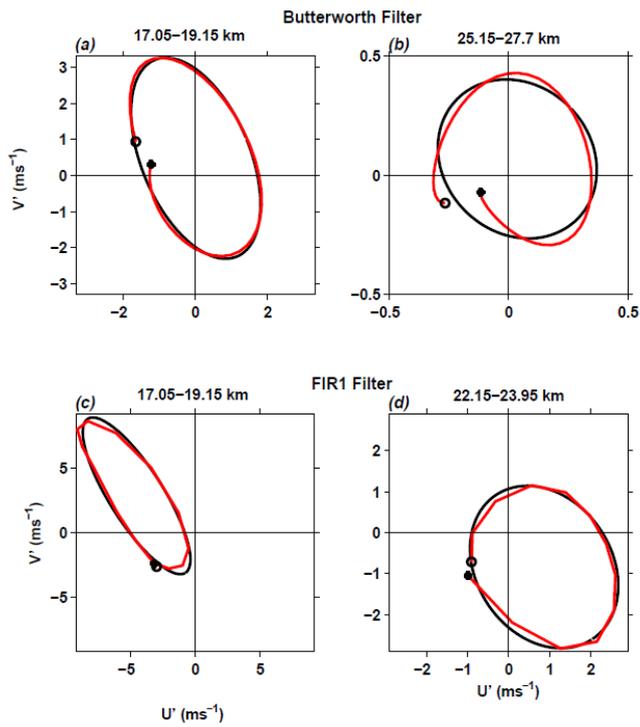
FIR1 Filter

(c) 17.05–19.15 km

(d) 22.15–23.95 km

Figure 4: Hodographs of horizontal wind fluctuations (ms⁻¹) obtained using Butterworth (a, b) and FIR1 (c, d) filters. An open circle and a solid circle in each hodograph indicate the lowest and highest altitudes, respectively. The thin curves represent the elliptical fits.
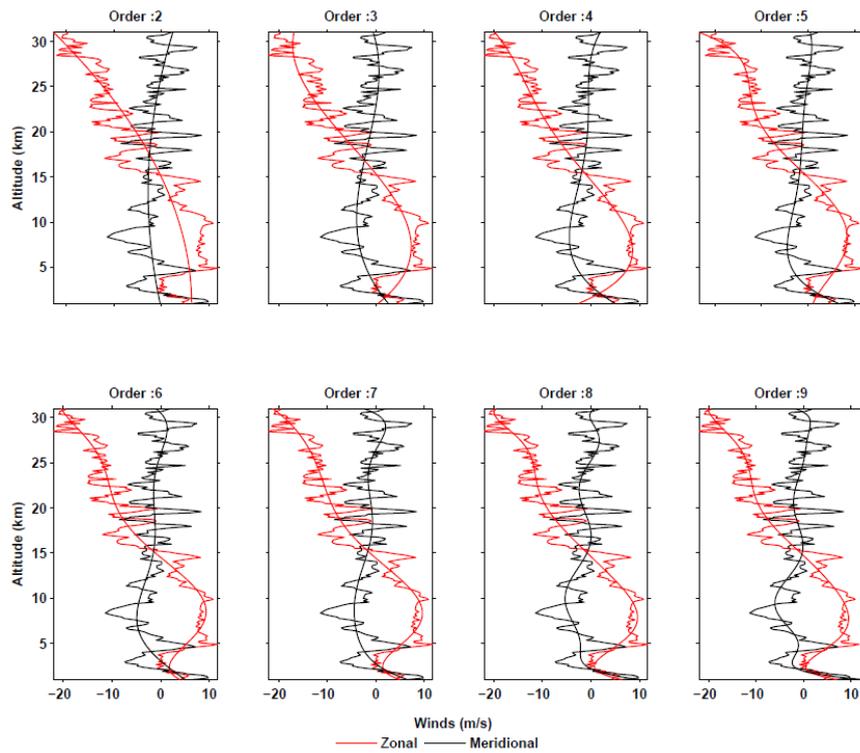
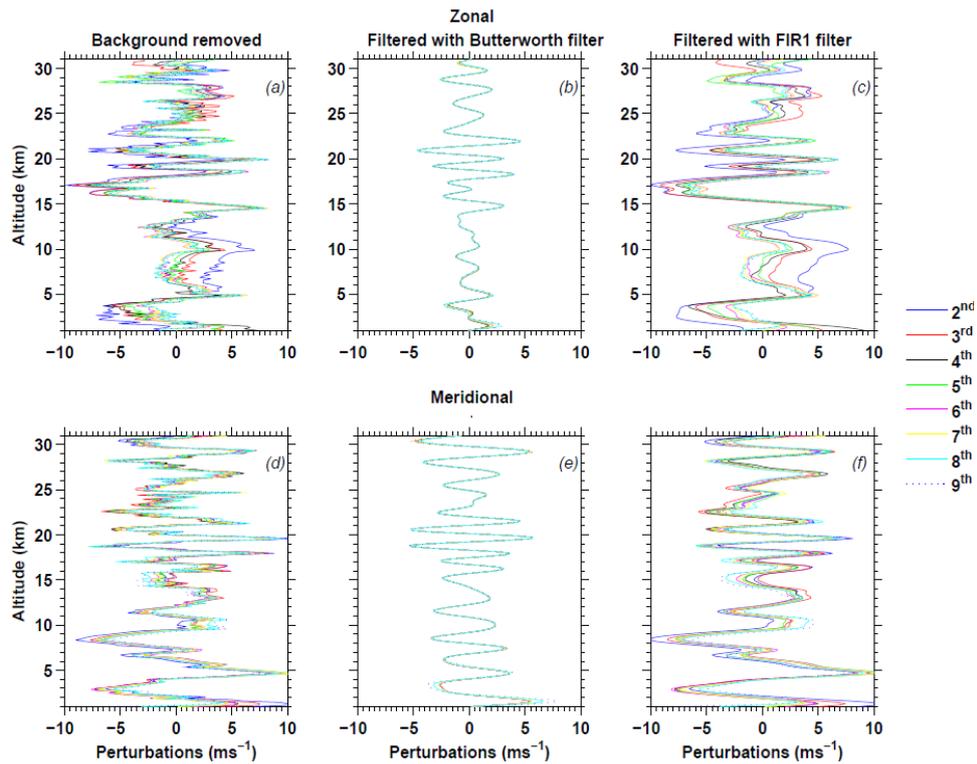**Figure 5: Profiles of zonal and meridional winds (ms^{-1}) and their fits with different orders.**

Figure 6: Upper panel: Vertical profiles of zonal wind fluctuations (ms^{-1}) after approximating the backgrounds with different order (2nd – 9th) polynomials (a) and filtering height-wise with Butterworth filter (b) and FIR1 filter (c). Lower panel: Same as upper panel but for meridional wind fluctuations.
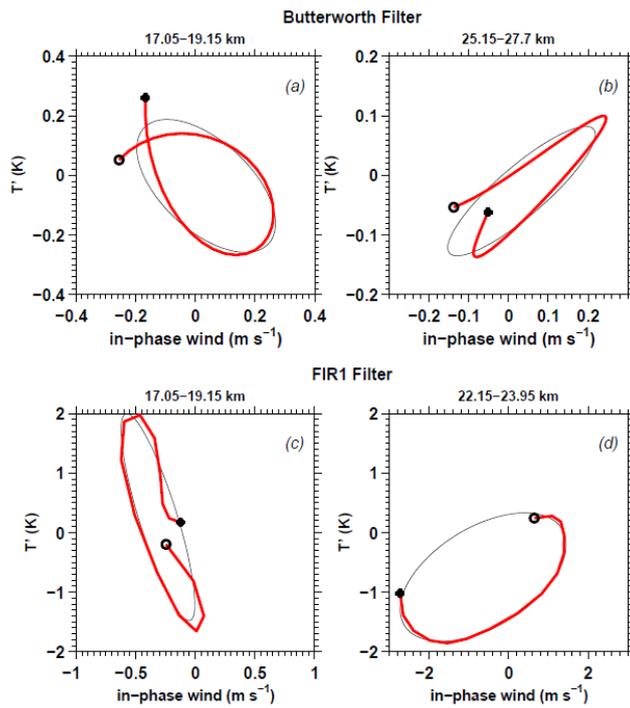
Figure 7: Hodographs of in-phase wind (ms^{-1}) verses temperature fluctuations (K) obtained using Butterworth (a, b) and FIR1 (c, d) filters. An open circle and a solid circle in each hodograph indicate the lowest and highest altitudes, respectively. The thin curves represent the elliptical fits.

5

Table 1: Comparison of IGW parameters using detrended time series fluctuations and obtained with different filters

Parameters	Butterworth filter	FIR1 filter
Horizontal wavelength (km)	569 – 1171	237 – 1209
Vertical wavelength (km)	2.0 – 2.8	1.5 – 3.5
Intrinsic Period (h)	20 – 28	10 – 30
Ratio of minor to major axis	0.44 – 0.76	0.35 – 0.87
Direction of propagation	South-East (58%)	South-East (55%)

Table 2: Comparison of IGW parameters using individual set of wind fluctuation profiles by removing the backgrounds with different order polynomial fits and using both the filters.

Parameters		Horizontal wavelength (km)	Vertical wavelength (km)	Intrinsic Period (h)	Ratio of minor to major axis	Direction of propagation
Filter	Order number					
Butterworth	2 to 9	423 – 986	2.0 – 2.6	16.0 – 25.0	0.34 – 0.71	South – East (52%)
FIR1	2	324 – 882	1.7 – 4.0	15.0 – 23.0	0.34 – 0.71	South – East (51%)
	3	472 – 827	1.7 – 4.0	17.3 – 23.9	0.32 – 0.71	South – East (58%)
	4	404 – 844	1.7 – 3.2	15.8 – 23.5	0.32 – 0.71	South – East (60%)
	5	273 – 1090	1.8 – 3.1	16.0 – 25.0	0.32 – 0.70	South – East (64%)
	6	361 – 905	1.7 – 4.0	15.8 – 24.7	0.30 – 0.69	South – East (61%)
	7	440 – 920	1.7 – 4.0	16.1 – 25.4	0.30 – 0.69	South – East (56%)
	8	360 – 878	1.8 – 3.1	16.0 – 25.0	0.32 – 0.68	South – East (55%)
	9	352 – 739	1.7 – 4.0	16.2 – 25.0	0.31 – 0.68	South – East (51%)